given in Figure 2, where energies of the orbitals of $MnCl_2$ with substantial d character are plotted against the bending angle (θ). The d_δ orbitals are degenerate at 180° but split and gently rise in energy for smaller values of θ. The d_π orbitals are also energetically degenerate at 180°, but one d_π component rises in energy rapidly for small values of θ while the other d_π component undergoes a gradual ascent. In contrast, the d_σ orbital decreases in energy as θ decreases.

The behavior of the d orbitals in Figure 2 as a function of θ can be contrasted with similar curves for previous calculations on ZnF_2[31] and MnH_2.[32] For both ZnF_2 and $MnCl_2$ the $F(2p_\pi)$ and $Cl(3p_\pi)$ orbitals are antibonding with respect to the metal d_π orbitals. Thus, as θ decreases, the d_π component that rises rapidly on bending is the result of the loss of a metal($3d_\pi$)–ligand(p_π) antibonding interaction coupled to an increasing ligand (σ) antibonding interaction, with the latter prevailing. These two effects lead to the destabilization of the d_π orbitals in both $MnCl_2$ and ZnF_2. For $MnCl_2$ the d_σ orbital energy *decreases* on bending but *increases* on bending for ZnF_2. This behavior can be attributed to both a larger antibonding interaction with the d_{z^2} orbital in ZnF_2 than in $MnCl_2$ and a stronger $Mn(d_{z^2}) + \lambda 4s$ mixing, which would favor bending. The situation for MnH_2 produces a Walsh diagram similar to that for $MnCl_2$, but the absence of π orbitals on H produces some differences.

It is possible to derive a qualitative model from Figure 2 to give useful information about the trends in geometry and electronic structure of other transition-metal dichlorides. A d^4 $CrCl_2$ molecule with electronic configuration $...1\delta_g^2 3\pi_g^2$ would most likely be linear.[33] Interestingly, experimental studies of high-temperature $CrCl_2$ and VCl_2 vapors[8] appear to point to bent structures for these molecules. This can be reationalized on the basis of Figure 2, supposing that the electronic configuration of $CrCl_2$ would not be $...1\delta_g^2 3\pi_g^2$ but rather $...1\delta_g^2 3\pi_g^1 9\sigma_g^1$. In this case an electron is removed from the d_{yz} orbital, which rises rapidly in energy on bending, and is placed in a d_{z^2} orbital, which decreases in energy upon bending. Thus the $CrCl_2$ molecule would favor a bent geometry with a lower total energy than for the linear configuration. The same reasoning is applicable to the d^3 VCl_2 molecule. In future work, we propose to investigate our model further and to determine the electronic structure of other transition-metal dichlorides.

Acknowledgment. One of us (M.H) expresses appreciation for the hospitality extended to her by the University of Connecticut and to the Research Foundation for financial support. A generous grant of computer time by the Department of Computer Systems of the University of Connecticut is also gratefully acknowledged. Finally, it is a pleasure to acknowledge fruitful discussions with D. Fox, H. F. Schaefer, III, T. A. Albright, and R. Bartram.

Registry No. $MnCl_2$, 7773-01-5.

(31) Yarkony, D. R.; Schaefer, H. F., III. *Chem. Phys. Lett.* **1972**, *15*, 514.
(32) Demuynck, J.; Schaefer, J. F. III. *J. Chem. Phys.* **1980**, *72*, 311.
(33) Garner, C. D.; Hillier, I. H.; Wood, C. *Inorg. Chem.* **1978**, *17*, 168.

Contribution from the Dipartimento di Chimica Inorganica e Struttura Molecolare, Università di Messina, 98100 Messina, Italy

Chemical Oxidation of Binuclear Rhodium(I) Complexes with Silver Salts. Synthesis and X-ray Crystal Structure of the Paramagnetic Rh_2^{5+} Formamidinate Complex $Rh_2(Form)_3(NO_3)_2$

Pasquale Piraino,* Giuseppe Bruno, Francesco Nicolò, Felice Faraone, and Sandra Lo Schiavo

Received February 25, 1985

The chemistry of the complexes characterized by the presence of Rh_2^{4+} core is still an attractive field of research, and a wealth of experimental data, complemented by theoretical studies, are available for such complexes.[1] In contrast, little is known on complexes containing the Rh_2^{5+} core mainly because these species have been rarely isolated.[2,3] These complexes in fact are generated when the Rh_2^{4+} derivatives $Rh_2(carboxylate)_4$ are electrochemically oxidized, undergoing a one-electron oxidation at a potential that is dependent on the electronic properties of the bridging ligands.[1] Recently Bear and co-workers synthesized the series of mixed-ligand Rh_2^{4+} complexes[4] $Rh_2(ac)_n(acam)_{4-n}$ (ac = $[O_2CCH_3]^-$, acam = $[HNOCCH_3]^-$, n = 0–4) showing that the redox potential for the Rh(II,II) ⇌ Rh(II,III) conversion is a function of the number of the acetamidate groups. On the other hand, it is known that the electrochemical oxidation of the trifluoroacetate derivative $Rh_2(O_2CCF_3)_4$ does not occur up to 1.8 V vs. SCE.[5] The existence of species containing the Rh_2^{4+} or Rh_2^{5+} cores is then determined from the donor properties of the bridging ligands. So a careful adjustment of the electronic density on the rhodium atoms by means of the appropriate ligands could permit the synthesis of complexes containing the Rh_2^{4+} or Rh_2^{5+} cores.

We have found a synthetic route that enabled us to synthesize the mixed-ligand complex $Rh_2(Form)_2(O_2CCF_3)_2(H_2O)_2$ (Form = $[p\text{-}MeC_6H_4NC(H)NC_6H_4Me\text{-}p]^-$) containing the Rh_2^{4+} core[6] and the mixed-valence complex $Rh_2(Form)_3(NO_3)_2$ containing the Rh_2^{5+} core. This method is based on the chemical oxidation with the appropriate silver salt of the Rh(I) formamidinate complex $[Rh(C_8H_{12})(Form)]_2$. In this paper we describe the synthesis, the spectroscopic properties, and the X-ray crystal structure of the complex $Rh_2(Form)_3(NO_3)_2$.

Experimental Section

Preparation of $Rh_2(Form)_3(NO_3)_2$. $[Rh(C_8H_{12})(Form)]_2$[7] (0.400 g, 0.46 mmol) was dissolved in 100 mL of a CH_2Cl_2–CH_3OH (1:1) mixture, and silver nitrate (0.156 g, 0.92 mmol) dissolved in water (1 mL) was added in the dark. The solution suddenly turned green while a gray precipitate of silver metal was formed. The mixture was stirred at room temperature for ≃4 h to effect reaction, indicated by the final blue-violet color. The solution was then filtered on a short Celite column to remove the silver, and the solvent was evaporated under reduced pressure until crystallization commenced. The deposition was completed by allowing the solution to stand overnight. The black-violet solid obtained was collected and crystallized from benzene–heptane, affording 0.250 g of complex (yield 63%). Anal. Calcd for $C_{45}H_{45}N_8O_6Rh_2$: C, 54.06; H, 4.53; N, 11.20; O, 9.60. Found: C, 54.23; H, 4.50; N, 10.91; O, 9.61.

X-ray Data Collection and Structure Refinement. Suitable black-violet crystals of the complex of cubic habit were obtained by slow evaporation from a benzene–heptane solution. A crystal of approximate dimensions 0.10 × 0.10 × 0.09 nm was selected and mounted on a Siemens-Stoe automatic four-circle diffractometer. Accurate unit-cell dimensions and crystal orientation matrices together with their estimated standard errors were obtained from least-squares refinement of the 2θ, ω, χ, and ϕ values of 25 carefully centered high-angle reflections using graphite-monochromated Mo Kα radiation (λ = 0.71069 Å). The complex crystallizes in the triclinic space group $P\bar{1}$, with a = 11.791 (1) Å, b = 13.066 (2) Å, c = 16.881 (4) Å, α = 110.69 (3)°, β = 92.89 (2)°, γ = 114.68 (3)°, V = 2149.96 Å^3, $F(000)$ = 1018, Z = 2, and D_{calcd} = 1.664 g cm^{-3}. X-ray data were collected at room temperature for all independent reflections in the range $3 \le 2\theta \le 50°$. An ω–θ scan technique was used for each reflection with a scan speed 0.03° s^{-1} and scan width 1.2°. No reflections were sufficiently intense to require the insertion of attenuators into the beam. Three standard reflections were monitored periodically during the

(1) (a) Felthouse, T. R. *Prog. Inorg. Chem.* **1982**, *20*, 109. (b) Boyer, E. B.; Robinson, S. D. *Coord. Chem. Rev.* **1983**, *50*, 109. (c) Cotton, F. A.; Walton, R. A. "Multiple Bonds between Metal Atoms"; Wiley-Interscience: New York, 1982; p 311.
(2) (a) Ziolkowski, J. S.; Moszner, M.; Glowiak, T. *J. Chem. Soc., Chem. Commun.* **1977**, 760. (b) Moszner, M.; Ziolkowski, J. S. *Transition Met. Chem. (Weinheim, Ger.)* **1982**, *7*, 351.
(3) Cannon, R. D.; Powell, D. B.; Sarawek, K.; Stilman, J. S. *J. Chem. Soc., Chem. Commun.* **1976**, 31.
(4) Zhu, T. P.; Ahsan, M. Q.; Malinski, T.; Kadish, K. M.; Bear, J. L. *Inorg. Chem.* **1984**, *23*, 2.
(5) Das, K.; Kadish, K. M.; Bear, J. L. *Inorg. Chem.* **1978**, *17*, 930.
(6) Manuscript in preparation.
(7) Piraino, P.; Tresoldi, G.; Faraone, F. *J. Organomet. Chem.* **1982**, *224*, 305.

0020-1669/85/1324-4760$01.50/0

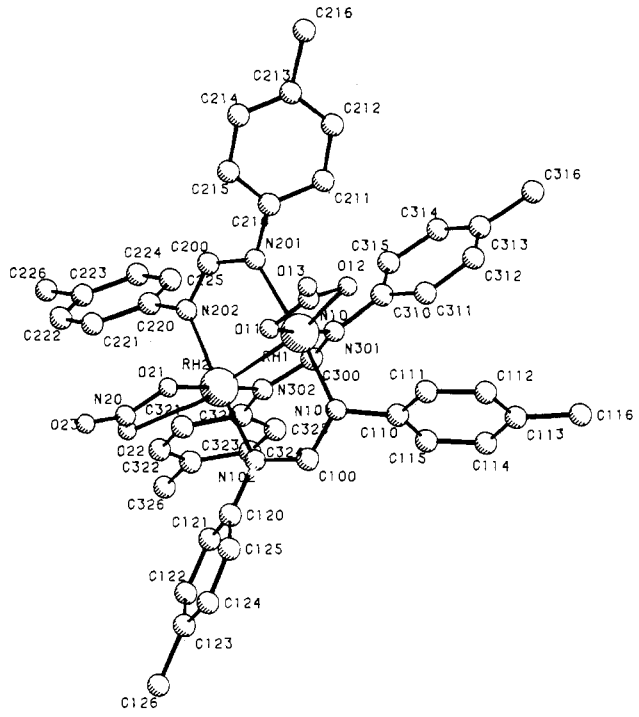

Figure 1. Molecular structure of $Rh_2(Form)_3(NO_3)_2$ with atomic labels.

course of the data collection as a check of crystal stability, and these varied by less than 3%. In the reduction of the data, Lorentz and polarization factors were applied, but no absorption correction was made due to the low absorption coefficient (μ = 8.106 cm^{-1}) and the fairly uniform dimension of the crystal. Of the 4690 independent reflections measured, 3245 having $I \geq 3\sigma(I)$ were used in all calculations. The structure was solved by interpretation of the Patterson map, which clearly indicated the positions of the two independent rhodium atoms. The refinement of the structural model, which was by the method of full-matrix least squares, was carried out, allowing the Rh, the nitrato group atoms, and N(101) and C(100) to vibrate anisotropically, while isotropic thermal parameters were applied to all non-hydrogen atoms. Hydrogen atoms were included in the scattering model in calculated idealized positions (C–H = 0.96 Å) with a common thermal parameter (B = 6 $Å^2$) but not varied.

Mean values of $w\Delta^2$ showed virtually no dependence on $(\sin\theta)/\lambda$ and $|F_o|$. Convergence was achieved at $R = (\sum||F_o| - |F_c||)/\sum F_o = 0.072$ and $R_w = [\sum w(|F_o| - |F_c|)^2/\sum w|F_o|^2]^{1/2} = 0.075$. The function minimized was $w\Delta^2$, in which $w = 1.821/(\sigma^2|F_o| + 0.003372|F_o|^2)$ and $\Delta = |F_o| - |F_c|$. Atomic scattering factors were taken from ref 8. Allowance was made for the anomalous scattering of rhodium, with use of $\Delta f'$ and $\Delta f''$ from ref 9. All the calculations were performed with the SHELX 76 set of programs[10] on the IBM 4341 computer of the Centro di Calcolo dell' Università di Messina. Distances associated with the tolyl fragments and nitrato groups (Table IV), hydrogen atom parameters (Table V), temperature factors (Table VI), and structure factors have been deposited as supplementary material.

Results and Discussion

Room-temperature oxidation of the Rh(I) formamidinate complex $[Rh(C_8H_{12})(Form)]_2$ with silver nitrate (ratio 1:2) rapidly affords silver metal while the solution turns immediately green and finally blue-violet. Workup of the resulting solution, as described in the Experimental Section, gave black-violet crystals of a complex formulated as $Rh_2(Form)_3(NO_3)_2$. In this complex the total formal oxidation number of the two rhodium atoms is increased by three units with respect to the starting complex. From the reaction mixture were isolated two byproducts, which we were not able to isolate in a pure form. The presence of these two species, probably Rh(I) or Rh(III) derivatives (their color is red) makes obscure the mechanism of the oxidation as well as the stoichiometry of the reaction.

The title complex, which has no known analogues, is remarkably stable to air. It dissolves, without chemical change, in benzene, diethyl ether, acetone, chlorinated solvents, and coordinating solvents such as CH_3CN and Me_2SO. The electronic spectrum, recorded in CH_2Cl_2, in the visible region shows an intense absorption with maximum at 518 nm (ϵ = 4000 M^{-1} cm^{-1}). This value is only slightly affected by using coordinating solvents. The assignment of this electronic transition, probably of a ligand-to-metal charge-transfer nature, as previously suggested,[11] is uncertain in the absence of theoretical studies. The infrared spectrum exhibits the N–C–N stretching frequency at 1520 cm^{-1}, a value that is indicative of extensive electronic delocalization.

The measurements of magnetic susceptibility show that the complex $Rh_2(Form)_3(NO_3)_2$ is paramagnetic. It exhibits a magnetic moment of 1.85 μ_B. This value is indicative of one unpaired electron per dimer unit and is in good agreement with the literature data.[1]

Table I. Selected Interatomic Distances (Å) and Angles (deg)

Rh(1)–Rh(2)	2.485 (1)		
Rh(2)–N(102)	2.012 (15)	Rh(1)–N(101)	2.034 (15)
Rh(2)–N(202)	2.041 (14)	Rh(1)–N(201)	2.047 (15)
Rh(2)–N(302)	1.946 (18)	Rh(1)–N(301)	1.985 (16)
Rh(2)–O(21)	2.086 (13)	Rh(1)–O(11)	2.090 (13)
Rh(2)–O(22)	2.382 (12)	Rh(1)–O(12)	2.287 (8)
N(102)–C(100)	1.337 (20)	N(101)–C(100)	1.339 (18)
N(102)–C(120)	1.411 (19)	N(101)–C(110)	1.460 (23)
N(202)–C(200)	1.280 (17)	N(201)–C(200)	1.333 (16)
N(202)–C(220)	1.438 (16)	N(201)–C(210)	1.413 (18)
N(302)–C(300)	1.361 (21)	N(301)–C(300)	1.293 (15)
N(302)–C(320)	1.418 (16)	N(301)–C(310)	1.437 (20)
Rh(1)–Rh(2)–O(21)	95.6 (3)	Rh(2)–Rh(1)–O(11)	99.0 (3)
Rh(1)–Rh(2)–O(22)	151.9 (4)	Rh(2)–Rh(1)–O(12)	156.2 (4)
Rh(1)–Rh(2)–N(202)	87.0 (3)	Rh(2)–Rh(1)–N(201)	88.1 (4)
Rh(1)–Rh(2)–N(102)	88.9 (4)	Rh(2)–Rh(1)–N(101)	86.9 (3)
Rh(1)–Rh(2)–N(302)	88.4 (4)	Rh(2)–Rh(1)–N(301)	86.1 (4)
Rh(1)–N(201)–C(200)	117.7 (9)	Rh(2)–N(202)–C(200)	120 (1)
Rh(1)–N(101)–C(100)	121 (1)	Rh(2)–N(102)–C(100)	120 (1)
Rh(1)–N(301)–C(300)	123 (1)	Rh(2)–N(302)–C(300)	121 (1)
O(11)–N(10)–O(12)	111 (1)	O(21)–N(20)–O(22)	116 (2)
Rh(1)–N(201)–C(210)	126 (1)	Rh(2)–N(202)–C(220)	122.3 (9)
Rh(1)–N(101)–C(110)	120.7 (9)	Rh(2)–N(102)–C(120)	127 (1)
Rh(1)–N(301)–C(310)	117 (1)	Rh(2)–N(302)–C(320)	123 (1)
N(202)–C(200)–N(201)	125 (1)		
N(102)–C(100)–N(101)	123 (1)		
N(302)–C(300)–N(301)	121 (1)		
O(11)–Rh(1)–O(12)	57.3 (4)		
O(21)–Rh(2)–O(22)	56.3 (5)		

Table II. Relevant Torsional Angles (deg)

N(201)–Rh(1)–Rh(2)–N(202)	7.7 (5)
N(101)–Rh(1)–Rh(2)–N(102)	6.7 (5)
N(301)–Rh(1)–Rh(2)–N(302)	6.0 (6)
O(11)–Rh(1)–Rh(2)–O(21)	5.1 (4)
N(101)–Rh(1)–Rh(2)–N(202)	−174.3 (5)
N(201)–Rh(1)–Rh(2)–N(102)	−171.3 (5)
O(11)–Rh(1)–Rh(2)–N(302)	−175.1 (5)
Rh(1)–N(201)–C(210)–C(211)	54 (2)
Rh(1)–N(301)–C(310)–C(311)	44 (2)
Rh(1)–N(101)–C(110)–C(111)	69 (2)
Rh(1)–O(11)–N(10)–O(13)	180 (1)
O(22)–Rh(2)–Rh(1)–O(12)	3 (1)
Rh(2)–O(21)–N(20)–O(23)	180 (1)
N(201)–C(200)–N(202)–C(220)	−159 (1)
N(202)–C(200)–N(201)–C(210)	6 (2)
N(102)–C(100)–N(101)–C(110)	21 (1)
N(101)–C(100)–N(102)–C(120)	−171 (1)
N(301)–C(300)–N(302)–C(320)	178 (1)
N(302)–C(300)–N(301)–C(310)	5 (1)

(8) "International Tables for X-ray Crystallography"; Kynoch Press: Birmingham, England, 1974; Vol. IV.
(9) Reisner, M. G.; Bernal, I.; Brunner, H.; Watcher, J. *J. Organomet. Chem.* **1977**, *137*, 329.
(10) Sheldrick, G. M. "SHELX 76 Computing System of Crystallography Programs"; University of Cambridge: Cambridge, England, 1976.
(11) Bear, J. L.; Zhu, T. P.; Malinski, T.; Dennis, A. M.; Kadish, K. M. *Inorg. Chem.* **1984**, *23*, 674.

Table III. Final Fractional Atomic Coordinates (×10⁴)

atom	x/a	y/b	z/c
Rh(1)	2775 (1)	1029 (1)	3062 (1)
Rh(2)	1788 (1)	-947 (1)	1737 (1)
O(11)	4658 (10)	1292 (9)	3262 (6)
O(12)	4377 (12)	2670 (9)	4209 (6)
O(13)	6275 (13)	2757 (13)	4300 (8)
N(10)	5181 (15)	2296 (12)	3967 (9)
N(20)	3001 (17)	-2208 (13)	1041 (9)
O(22)	1877 (12)	-2673 (10)	673 (7)
O(23)	3754 (14)	-2625 (13)	837 (8)
O(21)	3426 (10)	-1193 (9)	1721 (6)
N(101)	3145 (12)	1899 (10)	2246 (7)
C(100)	2909 (15)	1257 (13)	1385 (9)
N(102)	2410 (13)	26 (11)	1014 (7)
C(111)	4284 (15)	4140 (14)	3154 (9)
C(112)	4263 (16)	5278 (15)	3451 (10)
C(113)	3290 (16)	5424 (15)	3119 (10)
C(114)	2304 (16)	4405 (15)	2441 (10)
C(115)	2318 (16)	3266 (15)	2162 (10)
C(110)	3247 (15)	3132 (13)	2511 (9)
C(116)	3273 (17)	6657 (15)	3483 (12)
C(121)	1323 (14)	-1335 (13)	-495 (9)
C(122)	1283 (14)	-1808 (13)	-1375 (9)
C(123)	2367 (15)	-1344 (14)	-1660 (10)
C(124)	3495 (14)	-391 (13)	-1039 (9)
C(125)	3527 (14)	28 (13)	-176 (9)
C(120)	2408 (14)	-450 (13)	123 (9)
C(126)	2380 (20)	-1833 (17)	-2625 (10)
N(201)	2392 (12)	11 (11)	3790 (7)
C(200)	1667 (15)	-1211 (12)	3374 (9)
N(202)	1246 (12)	-1818 (10)	2548 (7)
C(211)	2645 (14)	1422 (13)	5270 (9)
C(212)	2990 (16)	1754 (15)	6153 (10)
C(213)	3593 (15)	1237 (15)	6488 (10)
C(214)	3850 (15)	343 (14)	5939 (10)
C(215)	3479 (14)	-15 (14)	5039 (9)
C(210)	2847 (14)	472 (13)	4698 (9)
C(216)	3965 (20)	1659 (18)	7469 (10)
C(221)	181 (15)	-4110 (14)	1684 (10)
C(222)	-967 (17)	-5224 (16)	1428 (11)
C(223)	-2021 (15)	-5280 (14)	1689 (10)
C(224)	-2028 (17)	-4237 (16)	2264 (11)
C(225)	-920 (16)	-3106 (15)	2539 (10)
C(220)	152 (14)	-3017 (13)	2268 (9)
C(226)	-3246 (20)	-6520 (16)	1381 (13)
N(301)	1030 (13)	900 (11)	2981 (7)
C(300)	61 (15)	44 (13)	2344 (9)
N(302)	196 (14)	-831 (11)	1680 (8)
C(311)	1717 (15)	2976 (14)	4104 (10)
C(312)	1515 (15)	3808 (13)	4811 (9)
C(313)	407 (15)	3431 (14)	5097 (10)
C(314)	-493 (17)	2217 (16)	4697 (11)
C(315)	-253 (15)	1386 (14)	4020 (10)
C(310)	837 (14)	1749 (13)	3708 (9)
C(316)	186 (21)	4345 (18)	5831 (11)
C(321)	-1014 (15)	-2912 (14)	549 (10)
C(322)	-2158 (15)	-3861 (14)	-69 (10)
C(323)	-3220 (14)	-3744 (13)	-240 (9)
C(324)	-3117 (15)	-2565 (14)	231 (10)
C(325)	-1999 (13)	-1582 (12)	853 (8)
C(320)	-940 (14)	-1747 (12)	1032 (9)
C(326)	-4404 (16)	-4769 (14)	-918 (10)

Figure 1 illustrates the molecular structure of the complex $Rh_2(Form)_3(NO_3)_2$ and atomic labeling scheme. Selected bond distances and angles are shown in Table I; some relevant torsional angles and the final fractional atomic coordinates are given in Tables II and III, respectively.

The molecular structure consists of three formamidinate bridging ligands symmetrically disposed about the Rh–Rh unit with the two bidentate nitrate groups unsymmetrically coordinated to each rhodium atom. The Rh–Rh bond distance of 2.485 (1) Å is quite long if compared with the distances found in the complex $[Rh_2(O_2CCH_3)_4(H_2O)_2]^{+}$ [2a] and most of the Rh_2^{4+} derivatives,[1] especially if we consider that the increased positive charge on the rhodium atoms of $Rh_2(Form)_3(NO_3)_2$ ought to increase the order bond. But the Rh–Rh separation in such complexes is dependent on the nature and the number of the bridging ligands. The reduced number and the different constraining effect of the bridging ligands can explain the longer Rh–Rh distance in the title complex.

The equatorial Rh(1)–O(11) and Rh(2)–O(21) bond lengths, respectively 2.090 (13) and 2.086 (13) Å, are significantly shorter than the axial Rh(1)–O(12) = 2.287 (8) Å and Rh(2)–O(22) = 2.382 (12) Å, in accordance with the high trans influence of the Rh–Rh bond. The very small O(11)–Rh(1)–O(12) = 57.3 (4)° and O(21)–Rh(2)–O(22) = 56.3 (5)° bond angles and the values of 95.6 (3) and 99.0 (3)° for the angles Rh(1)–Rh(2)–O(21) and Rh(2)–Rh(1)–O(11) are clearly imposed by the bidentate coordination of the nitrate groups which are then responsible for the distortion from the normal octahedral coordination around each rhodium atom.

Each rhodium atom completes its coordination with three nitrogen atoms of the bridging ligands. The two formamidinate groups in transoid positions exhibit a mean Rh–N distance of 2.033 Å while the Rh–N distances of the third bridging ligand are significantly shorter (Rh(2)–N(302) = 1.946 (18) Å, Rh(1)–N(301) = 1.985 (16) Å). All the five-membered rings Rh–Rh–N–C–N deviate from the planarity and are twisted by an average of 6.35° (see Table II) from the eclipsed conformation. The ring C–N distances show considerable double-bond character, indicating that extensive delocalization occurs within the fragment N–C–N.

The symmetrical mixed-valence complex $Rh_2(Form)_3(NO_3)_2$ lies within the Robin and Day class II or III-A compounds,[12] and spectroscopic evidence is necessary to determine whether the oxidation states are integral (class II) or not (class III-A). However, we suspect, on the basis of the X-ray structural data, which show the symmetrical arrangement of the five anionic ligands around each rhodium atom, that in the title complex the rhodium sites are equivalent. This implies that it is not possible to locate the unpaired electron on one of the two rhodium atoms and that the formal oxidation state for each rhodium atom is 2.5.

Acknowledgment. We thank the CNR and the Public Education Ministry for financial support.

Registry No. $Rh_2(Form)_3(NO_3)_2$, 99416-57-6; $[Rh(C_8H_{12})(Form)]_2$, 81229-43-8; Rh, 7440-16-6.

Supplementary Material Available: Listings of interatomic distances and angles associated with the tolyl fragments and nitrato groups (Table IV), hydrogen atom parameters (Table V), temperature factors (Table VI), and structure factors (22 pages). Ordering information is given on any current masthead page.

(12) Robin, M. B.; Day, P. *Adv. Inorg. Chem. Radiochem.* **1967**, *10*, 247.

Contribution from the Chemistry Department, University of Tasmania, Hobart, TAS 7001, Australia

Interpretation of Copper(II) Hyperfine Parameters

Michael A. Hitchman

Received April 16, 1985

The effects of hyperfine coupling in EPR spectroscopy were first observed during the study of a copper(II) complex,[1] and these data provided the impetus for the derivation of the basic ex-

(1) Penrose, R. P. *Nature (London)* **1949**, *163*, 992.

0020-1669/85/1324-4762$01.50/0